J. Cent. South Univ. (2014) 21: 381−386
DOI: 10.1007/s11771-014-1951-2

Springer

Kinematical analysis of highway tunnel collapse using nonlinear failure criterion

YANG Xiao-li(杨小礼), YANG Zi-han(杨子汉), PAN Qiu-jing(潘秋景), LI Yu-lin(李育林)

School of Civil Engineering, Central South University, Changsha 410075, China

Abstract: For different kinds of rocks, the collapse range of tunnel was studied in the previously published literature. However, some tunnels were buried in soils, and test data showed that the strength envelopes of the soils followed power-law failure criterion. In this work, deep buried highway tunnel with large section was taken as objective, and the basic expressions of collapse shape and region were deduced for the highway tunnels in soils, based on kinematical approach and power-law failure criterion. In order to see the effectiveness of the proposed expressions, the solutions presented in this work agree well with previous results if the nonlinear failure criterion is reduced to a linear Mohr-Coulomb failure criterion. The present results are compared with practical projects and tunnel design code. The numerical results show that the height and width of tunnel collapse are greatly affected by the nonlinear criterion for the tunnel in soil.

Key words: upper bound theorem; tunnel collapse; highway tunnel; nonlinear failure criterion

1 Introduction

Many highway tunnels were built with a three-centered circular cross section in soils, thereby the significance of researches on the collapse pattern of circle tunnel was demonstrated in theory and practice. In geotechnical engineering, the research on failure mechanism, shape and region of tunnel collapse was complex and intractable, because the randomness of rock mechanics and the special geotectonic phenomena such as rock stratification, joint, fracture and so on, could bring about great difficulties for the research.

The methods for failure mechanism research include limit equilibrium method, slip line method and limit analysis method. LECA and DORMIEUX [1] built a three-dimensional failure model for sandy soil. The mechanism was improved by SOUBRA [2−3]. In the improved model, a series of slide mass, which intersected with the top of working face, were applied to simulate the smooth transition between the two cones. Thus, a superior upper bound solution could be obtained. The working face stabilization of shallow buried tunnel in three dimensions was studied by SUBRIN and WONG [4] with upper bound method, and a distinguishing failure model was proposed. SLOAN and ASSADI [5] put forward a model consisting of seven rigid slide bodies for shallow buried tunnel under impervious soft clay. As consisting of seven parameters, the failure model had a more flexible failure surface and could accurately show the soil character of sidewall. WANG [6] presented two failure models, the arch interlayer mechanism and the logarithm spiral interlayer mechanism, based on power-law criterion. And the models were optimized so as to analyze the influence of parameter on the location of fracture surface. Based on the Hoek-Brown criterion, FRALDI et al [7−9] first deduced the theoretical failure pattern and range of rectangular tunnel, and generalized the theory to arbitrary tunnel. Limit analysis and limit equilibrium methods were used to determine the collapse shape and scope of shallow tunnel [10−15].

For the problem of tunnel collapse, there were many theoretical researches aimed at the stability of rock pressure during the excavation [16−19]. The researches about the mechanism, shape and region were few. Therefore, the shape and magnitude of circular tunnel would be conducted in this work, based on the nonlinear power-law criterion and the upper bound theorem.

2 Power-law failure criterion

The constitutive equation of power-law failure criterion was:

Foundation item: Project(2013CB036004) supported by the National Basic Research Program of China; Project(51378510) supported by the National Natural Science Foundation of China
Received date: 2012−07−30; **Accepted date:** 2012−12−20
Corresponding author: YANG Xiao-li; Professor PhD; Tel: +86−14789933669; E-mail: yangky@aliyun.com

$$\tau_n = C_0(1+\frac{\sigma_n}{\sigma_t})^{1/m} \quad \{m \in (1,+\infty),\ \sigma_t \geq 0,\ C_0 \geq 0\} \tag{1}$$

where σ_n and τ_n are normal stress and shear stress, respectively; C_0 is the initial cohesion; m is nonlinear coefficient which could be obtained by experiment and σ_t is the tensile stress. When m=1, Eq. (1) becomes linear Mohr-Coulomb failure criterion:

$$\tau_n = C_0 + \frac{C_0}{\sigma_t}\sigma_n = c + \sigma_n \tan\phi \tag{2}$$

where $\{C_0 = c, \frac{C_0}{\sigma_t} = \tan\phi\}$

Due to the associated flow rule material, its plastic potential function f could be expressed as

$$f = \tau_n - C_0(1+\sigma_n/\sigma_t)^{1/m} \tag{3}$$

For the plastic flow material, the relationship between the yield stress and plastic strain was unclear, but the relationship between the yield stress and plastic strain rate was determined by flow rule. So, the functions of plastic normal strain $\dot{\varepsilon}_n$ and plastic shear strain $\dot{\gamma}_n$ were

$$\dot{\varepsilon}_n = \lambda\frac{\partial f}{\partial\sigma_n} = -\frac{\lambda C_0}{m\sigma_t}(1+\frac{\sigma_n}{\sigma_t})^{\frac{1-m}{m}} \tag{4}$$

$$\dot{\gamma}_n = \lambda\frac{\partial f}{\partial\tau_n} = \lambda \tag{5}$$

where λ is proportionality factor.

3 Upper bound solution

3.1 Range of tunnel collapse

For the circular tunnel as shown in Fig. 1, the distance from the tunnel centre to the origin of coordinate was $h_1 = \sqrt{R^2 - L^2}$, so the expression of tunnel profilogram is

$$c(x) = h_1 - \sqrt{R^2 - x^2} \tag{6}$$

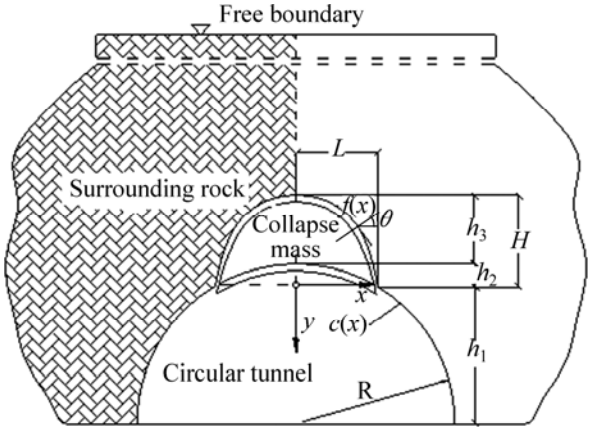

Fig. 1 Collapse diagram of circular tunnel

Meanwhile, the expression of σ_n could be derived from Eq. (4) as

$$-\frac{C_0}{m\sigma_t}(1+\frac{\sigma_n}{\sigma_t})^{\frac{1-m}{m}} = -\frac{1}{f'(x)} \tag{7}$$

$$\sigma_n = \sigma_t(\frac{m\sigma_t}{f'(x)C_0})^{\frac{m}{1-m}} - \sigma_t \tag{8}$$

According to the upper bound theorem, the unit internal energy dissipation power of collapse separation surface per unit length could be obtained.

$$\dot{D}_i = \sigma_n\dot{\varepsilon}_n + \tau_n\dot{\gamma}_n = \{[-\sigma_t + \sigma_t^{\frac{1}{1-m}}C_0^{\frac{m}{m-1}}(\frac{1}{m})^{\frac{m}{m-1}} \cdot (1-m)f'(x)^{\frac{m}{m-1}}]/[w\sqrt{1+f'(x)^2}]\}\dot{u} \tag{9}$$

And the gravity power of collapse separation region per unit length was

$$\dot{W}_e = \{\gamma[f(x)-c(x)]\}\dot{u} \tag{10}$$

Based on the hypothetic collapse mechanism, the internal energy dissipation power and the gravity power had been determined. According to the upper bound method, the internal power was equal to the external power, thereby setting up the work equation as bellow, where only half the collapse region had been considered due to its symmetrical shape.

$$\dot{D}[f(x),f'(x),x] = \int_0^s \dot{D}_i\mathrm{d}s - \int_0^L \dot{W}_e\mathrm{d}x = \int_0^L(\dot{D}_i\sqrt{1+f'(x)^2} - \dot{W}_e)\mathrm{d}x = \int_0^L \Lambda[f(x),f'(x),x]\mathrm{d}x \tag{11}$$

where $\mathrm{d}s = \sqrt{1+f'(x)^2}\,\mathrm{d}x$ represents the length of an infinitesimal element on curve $f(x)$, S is the length of curve $f(x)$ on the right side, L is the projection of S on x-axis, which is also the half width of tunnel collapse. $\Lambda = \Lambda[f(x),f'(x),x]$ is a given function, expressed as

$$\Lambda[f(x),f'(x),x] = \dot{u}\{\gamma[f(x)-c(x)] - \sigma_t + \sigma_t^{\frac{1}{1-m}}C_0^{\frac{m}{m-1}}(\frac{1}{m})^{\frac{m}{m-1}}(1-m)f'(x)^{\frac{m}{m-1}}\} \tag{12}$$

Based on this tunnel collapse mechanism, the shape of collapse, defined as $y=f(x)$, was still unknown. According to the upper bound method, in order to get the minimum load of the failure mechanism, the external solution of $\Lambda = \Lambda[f(x),f'(x),x]$ should be calculated. And finally the function of $f(x)$, which could meet with the minimum upper bound solution, was obtained.

Solving the external value of Eq. (11) with variation method, the functions bellow should be satisfied:

$$\delta\dot{D} = \delta\dot{D}[f(x),f'(x),x] = 0$$

$$\frac{\partial \Lambda}{\partial f(x)}-\frac{\partial}{\partial x}(\frac{\partial \Lambda}{\partial f'(x)})=0 \tag{13}$$

From Eq. (12), it could be inferred that

$$\frac{\partial \Lambda}{\partial f(x)}=-\gamma\dot{u}\frac{\partial \Lambda}{\partial f'(x)}=\sigma_{\mathrm{t}}^{\frac{1}{1-m}}C_0^{\frac{m}{m-1}}(\frac{1}{m})^{\frac{m}{m-1}}\cdot$$
$$(1-m)(\frac{m}{m-1})f'(x)^{\frac{1}{m-1}}\frac{\partial}{\partial x}(\frac{\partial \Lambda}{\partial f'(x)})=$$
$$\psi f'(x)^{\frac{2-m}{m-1}}f(x)'' \tag{14}$$

where $\psi=\sigma_{\mathrm{t}}^{\frac{1}{1-m}}C_0^{\frac{m}{m-1}}(\frac{1}{m})^{\frac{m}{m-1}}(\frac{m}{m-1})>0$.

Substitute Eq. (14) into Eq. (13), the following expression is obtained:

$$\delta\dot{D}=0\Rightarrow\dot{u}[\psi f'(x)^{\frac{2-m}{m-1}}f(x)''-\gamma]=0 \tag{15}$$

The equation above was a second-order differential equation. If $f'(x)$ first integrated, the equation above turned to be:

$$\psi(m-1)f'(x)^{(\frac{1}{m-1})}-\gamma x-\tau_0=0 \tag{16}$$

Equation (16) is a first-order differential equation, from which the expression of $f'(x)$ could be deduced:

$$f'(x)=[\psi(m-1)]^{1-m}(\gamma x+\tau_0)^{m-1} \tag{17}$$

where τ_0 is a constant, which is determined with some constraint conditions. On the point x=0, y=−h, the shear stress, by asymmetry, did not exist. Therefore, one of the constraint conditions could be obtained:

$$\tau_{xy}(x=0,y=-h)=0 \tag{18}$$

At the same time, the relationship of stresses in the elasticity mechanism is

$$\tau_{xy}=\tau_{\mathrm{n}}\cos(2\theta)-\frac{1}{2}\sigma_{\mathrm{n}}\sin(2\theta) \tag{19}$$

$$\cos(2\theta)=\frac{f'(x)^2-1}{f'(x)^2+1};\ \frac{1}{2}\sin(2\theta)=\frac{f'(x)}{f'(x)^2+1} \tag{20}$$

As x=0, Eq. (17) could be rewritten as

$$\cot\theta\big|_{x=0}=f'(x=0)=[\psi(m-1)]^{1-m}\tau_0^{m-1}=Q\tau_0^{m-1} \tag{21}$$

where $Q=[\psi(m-1)]^{1-m}$. Then, substituting Eq. (21) into Eq. (19), the value of τ_0 could be solved:

$$(Q^2\tau_0^{2m-2}+1)^{-1}\{\tau_0(Q^2\tau_0^{2m-2}-1)+[\sigma_{\mathrm{t}}-$$
$$\sigma_{\mathrm{t}}(\frac{m\sigma_{\mathrm{t}}}{Q^2\tau_0^{2m-2}C_0})^{\frac{m}{1-m}}]Q\tau_0^{m-1}\}=0\Rightarrow\tau_0=0 \tag{22}$$

As τ_0=0, Eq. (17) could be simplified as

$$f'(x)=[\psi(m-1)]^{1-m}(\gamma x)^{m-1} \tag{23}$$

Integrating Eq. (23) is for the second time, and the result is the expression of $f(x)$:

$$f(x)=\frac{1}{m}[\psi(m-1)]^{1-m}\gamma^{m-1}x^m-H=k(x+\frac{\tau_0}{\gamma})^m-H \tag{24}$$

where $k=\frac{1}{m}[\psi(m-1)]^{1-m}\gamma^{m-1}=\sigma_{\mathrm{t}}C_0^{-m}\gamma^{m-1}$, and as shown in Fig. 1, H is the maximum total collapse height of circular tunnel, while h_2 is the maximum collapse height of tunnel arch, h_3 is the height between the top of tunnel and collapse mass. Then,

$$h_2=R-h_1=R-\sqrt{R^2-L^2},h_3=H-h_2 \tag{25}$$

From Fig. 1, it was found that, when x=L, y=$f(x)$=0. Taking the equation into Eq. (24), the maximum collapse width (L) and maximum collapse height (H) could be calculated.

$$f(x)=kx^m-H=0\Rightarrow H=kL^m,\ L=(\frac{H}{k})^{\frac{1}{m}} \tag{26}$$

Equation (12) could be rewritten by substitution of Eqs. (23) and (24):

$$\Lambda=[\gamma c(x)+\alpha-\beta x^m]\dot{u} \tag{27}$$

$$\alpha=\gamma H-\sigma_{\mathrm{t}},\ \beta=\gamma km \tag{28}$$

Substituting Eqs. (27) and (28) into Eq. (11), then taking the integration of x, the following expression is obtained:

$$\dot{D}=\int_0^L\Lambda\mathrm{d}x=\{[\int_0^L\gamma c(x)\mathrm{d}x]+\alpha L-\beta\frac{1}{m+1}L^{m+1}\}\dot{u}=$$
$$\dot{u}L(p+\alpha-\beta\frac{1}{m+1}L^m) \tag{29}$$

where

$$p=\frac{1}{L}\int_0^L\gamma c(x)\mathrm{d}x \tag{30}$$

After the Eqs. (29) and (30) being simplified and solved, the solution is

$$\dot{D}=0\Rightarrow p+\alpha-\beta\frac{1}{m+1}L^m=0\Rightarrow p+\alpha-$$
$$\beta\frac{1}{m+1}(\frac{H}{k})=0\Rightarrow H=\frac{\sigma_{\mathrm{t}}-p}{\gamma}(m+1) \tag{31}$$

$$L=(\frac{H}{k})^{\frac{1}{m}}=[\frac{\sigma_{\mathrm{t}}-p}{k\gamma}(m+1)]^{\frac{1}{m}}=$$
$$\frac{C_0(m+1)^{\frac{1}{m}}\sigma_{\mathrm{t}}^{-\frac{1}{m}}(\sigma_{\mathrm{t}}-p)^{\frac{1}{m}}}{\gamma} \tag{32}$$

Applying the function of collapse shape of circular tunnel, i.e., Eq. (6) to Eq. (30), the expression of p is

$$p=\frac{1}{L}\int_0^L \rho c(x)\mathrm{d}x=\frac{\gamma R^2}{2L}(\arcsin\frac{L}{R}-\frac{L\sqrt{R^2-L^2}}{R^2}) \quad (33)$$

Finally, the function of total weight of circular tunnel collapse could be settled:

$$P=-2\int_0^L \gamma[f(x)-c(x)]\mathrm{d}x=2\gamma L(\frac{mH}{m+1}+\frac{p}{\gamma}) \quad (34)$$

3.2 Upper bound solution of linear failure criterion

The linear failure criterion was still employed by many engineering calculation software, and circular tunnel was widely used. Therefore, in this work, the result under linear Mohr-Coulomb failure criterion was provided for the future calculation and design as important reference.

Substituting m=1 into Eqs. (26), (31) and (32), the results are of linear criterion:

$$f(x)\big|_{m=1}=kx^m-H=x\cot\phi-2c\gamma^{-1}\cot\phi+2\gamma^{-1}p \quad (35)$$

$$H\big|_{m=1}=\frac{\sigma_t-p}{\gamma}(m+1)=2c\gamma^{-1}\cot\phi-2\gamma^{-1}p \quad (36)$$

$$L\big|_{m=1}=\frac{C_0(m+1)^{\frac{1}{m}}\sigma_t^{-\frac{1}{m}}(\sigma_t-p)^{\frac{1}{m}}}{\gamma}=2\gamma^{-1}C_0(1-\frac{p}{\sigma_t}) \quad (37)$$

Equations (35)−(37) agree well with previous results if the nonlinear failure criterion is reduced to a linear Mohr-Coulomb failure criterion.

4 Comparison with practical engineering

In order to verify the solutions above, the parameters of practical engineering were taken into the equations derived, and the results of collapse height and width were compared with the real collapse data.

Example 1 happened in Dahua Mount Tunnel [16], which belonged to Yunwu Highway, located in Fuyun, Guangdong Province, China. It was a double-lane tunnel with separate up and down lines. Its location had a complicated rock condition, alternating with carboniferous limestone and sandstone schist. On 17th May, 2007, a massive collapse took place at mileage LK42+177. The collapse height was about 8−10 m, and width was about 8 m.

Example 2 was Leigong Mount Tunnel [17], located at Longgang District from Kuiyong Town to Dapengshuitou Section, in Shenzheng. The sedimentary rocks in this district had complicated geologic condition, which mainly comprised Quaternary residual soil and Carboniferous sandstone, and abundant with groundwater. On February 29, 2000, a tunnel collapse, which was 2.2−8 m high and 7−9 m wide, happened at the right-side entrance. Owing to the timely treatment, the collapse did not further expand.

Substituting the parameters in Table 1 and Table 2 into Eqs. (36) and (37), the maximum collapse height and width could be calculated, respectively, which were 7.9 m and 8 m for Dahua Mount Tunnel, and 6.5 m and 6.6 m for Leigong Mount Tunnel. The calculation results were slightly smaller than the measured data, because only the gravity was considered in the calculation, but the other loads such as seepage pressure from the groundwater, though small, also promote the expansion of collapse. Consequently, the correctness and effectiveness of the proposed method could be verified in the comparison.

5 Comparison with tunnel design code

In the Code for Design of Road Tunnel, the equivalent load height (h_q) was defined to divide the deep tunnel and shallow tunnel, also called average collapse height. Its function was:

$$h_q=0.45\times 2^{S-1}\omega \quad (38)$$

where S is the rock level of cavity, and ω is influence coefficient of span, which could be calculated by

$$\omega=1+i(B_t-5) \quad (39)$$

where B_t (m) is the width of cavity, i is the load gradient of vertical uniform pressure when B_t increased or decreased by 1 m from B_t=5 m. When B_t <5 m, i=0.2; when B_t=5−15 m, i=0.1; when B_t>15 m, i could be referred to be 0.1.

Taking the V-level surrounding rock as example, the collapse height of circular tunnel with arch radius of was calculated as 6 m. The calculation result of tunnel design norm (normative collapse height) was h_q=0.45×2^4×1.1=

Table 1 Parameters of collapse tunnel

Name of tunnel	Rock level	Unit weight, γ/(kN·m^{-3})	Elastic modulus, E/GPa	Poisson ratio, ν	Internal friction angle, φ/(°)	Cohesion, c/MPa
Dahua Mount Tunnel	V	20	1.2	0.39	22	0.06
Leigong Mount Tunnel	V	20	1.4	0.38	26	0.04

7.92 m. While the result of Eq. (36) could be got by substituting the data in Table 3, and collapse height H=8.3 m.

Table 2 Parameters for calculation

Name of tunnel	C_0/MPa	σ_t/MPa	γ/(kN·m^{-3})	R/m
Dahua Mount Tunnel	0.05	0.12	20	5.5
Leigong Mount Tunnel	0.04	0.082	20	6

Table 3 Parameters of V surrounding rock

C_0/MPa	σ_t/MPa	γ/(kN·m^{-3})	R/m
0.055	0.108	20	6

In the comparison, the results are close, which indicate the reliability and feasibility of the new method proposed in this work and could be adopted by designer as reference and guidance in the tunnel engineering.

6 Parameters influence analysis

6.1 Influence of nonlinear coefficient on collapse range

The parameters chosen in the calculation are as follows: σ_t=30 kPa, C_0=40 kPa, R=4 m, γ=22 kN/m^3, while m, as the variable, has a series of values which are 1.0, 1.2, 1.4, 1.6, 1.8, 2.0. After the maximum collapse height (H), width (L), contour parameters (h_1, h_2, h_3) and weight (P) are calculated, the shape of tunnel collapse can be outlined basically, which is shown in Fig. 2.

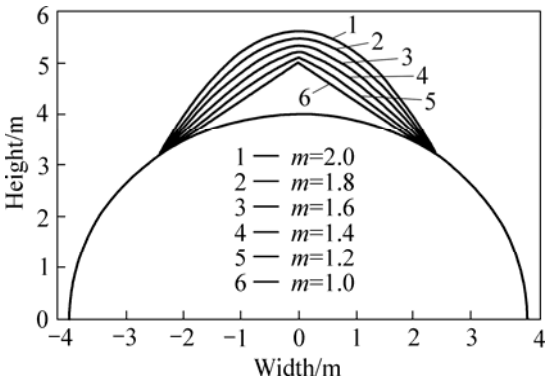

Fig. 2 Collapse contours under different nonlinear coefficients

It is indicated in Fig. 2 that the curvature of the outline of tunnel collapse increases with the increase of m, and so does the collapse height and width, which manifests that the collapse range is enlarged under bigger nonlinear coefficient.

6.2 Influence of axial tensile stress on collapse range

The parameters chosen in the calculation are as follows: m=1.6, C_0=40 kPa, R=4 m, γ=22 kN/m^3, while σ_t, as the variable, has a series of values which are 25, 27.5, 30, 32.5 and 35 kPa. The shape of tunnel collapse varying with the value of σ_t has been depicted in Fig. 3.

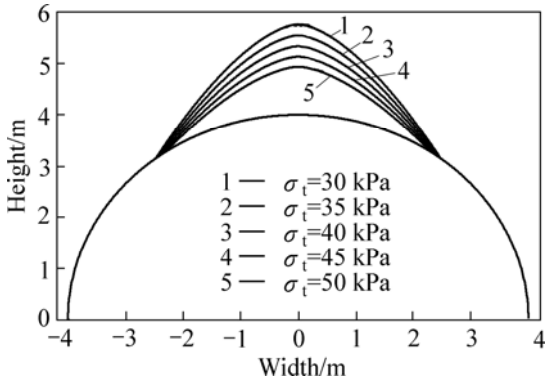

Fig. 3 Collapse contours under different axial tensile stresses

From Fig. 3, it is found that the curvature of the outline of tunnel collapse increases with the increase of σ_t, and so does the collapse height and width, which manifests that the collapse range will expand with the growth of axial tensile stress.

6.3 Influence of initial cohesion on collapse range

The parameters chosen in the calculation are as follows: σ_t=30 kPa, m=1.6, R=4 m, γ=22 kN/m^3, while C_0, as the variable, has a series of values which are 30, 35, 40, 45 and 50 kPa. The shape of tunnel collapse varying with the value of C_0 has been depicted in Fig. 4.

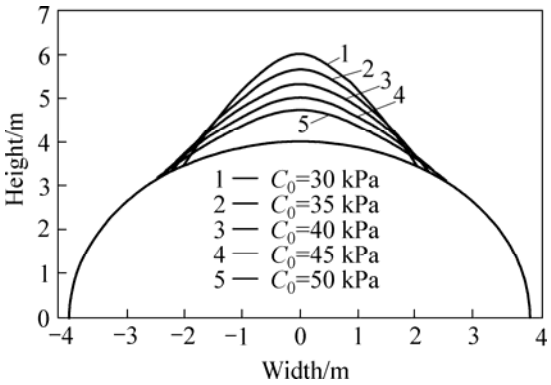

Fig. 4 Collapse contours under different initial cohesion

It is shown in Fig. 4 that the curvature of collapse outline and the collapse height decreases with the increase of C_0, but the collapse width becomes wider, which means that the collapse shape is much flatter when the initial cohesion becomes bigger.

6.4 Influence of tunnel arch radius on collapse range

The parameters chosen in the calculation are as follows: σ_t=30 kPa, C_0=40 kPa, m=1.6, γ=22 kN/m^3, while R, as the variable, has a series of values which are 3, 3.5, 4, 4.5 and 5 m. The shape of tunnel collapse

varying with the value of R has been depicted in Fig. 5.

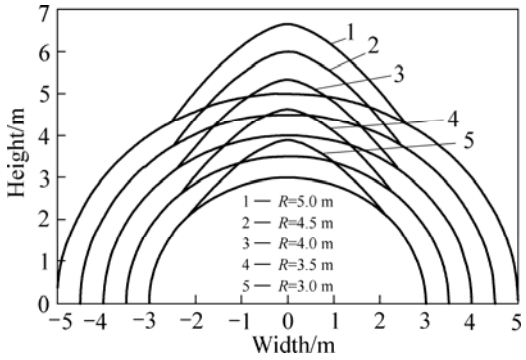

Fig. 5 Collapse contour under different tunnel arch radii

As shown in Fig. 5, the collapse height and width are growing up with the increase of R, that is, the range of tunnel collapse is bigger.

7 Conclusions

1) Based on the upper bound theorem and power-law criterion, the collapse range of circular tunnel is derived and compared with that of rectangular tunnel under the same failure criterion. The reasonability of the new method proposed in this work can be verified. Moreover, the equations of feature parameters which can delineate the collapse shape, such as collapse height and width, the maximum collapse height of tunnel arch, the height between the top of tunnel and collapse mass, are deduced.

2) By comparison with the practical engineering, the results of calculation are basically the same as the measured data of collapse feature. It indicates the correctness and feasibility of the equations are obtained here.

3) The diagram of tunnel collapse under various kinds of parameters has been outlined, so as to analyze the influence of parameters on the range and shape of circular tunnel. With the increase of nonlinear coefficient, axial tensile stress and tunnel arch radius, the collapse height and collapse width are higher and wider. With the increase of initial cohesion, the collapse range becomes bigger. The collapse height is reduced, but the collapse width increases. The shape of tunnel collapse is flat.

References

[1] LECA E, DORMIEUX L. Upper and lower bound solutions for the face stability of shallow circular tunnels in frictional materials [J]. International Journal of Rock Mechanics and Mining Sciences, 1991, 28(4): 255−236.

[2] SOUBRA A H, DIAS D. Three-dimensional face stability analysis of circular tunnels by a kinematical approach [J]. Geotechqiuue, 2008, 30(5): 894−901.

[3] SOUBRA A H. Three-dimensional face stability analysis of shallow circular tunnels [C]// International Conference on Geotechnical and Geological Engineering. Melbourne, Australia, 2000, 19−24.

[4] SUBRIN D, WONG H. Tunnel face stability in frictional material: A new 3D failure mechanism [J]. Comptes Rendus Mécanique, 2002, 330(7): 513−519.

[5] SLOAN S W, ASSADI A. Undrained stability of a square tunnel in a soil whose strength increases linearly with depth [J]. Computers and Geotechnics, 1991, 12(4): 321−346.

[6] WANG Z W. Supporting pressures of shallow tunnels with nonlinear failure criterion [D]. Changsha: Central South University, 2010. (in Chinese)

[7] FRALDI M, GUARRACINO F. Analytical solutions for collapse mechanisms in tunnels with arbitrary cross sections [J]. International Journal of Solids and Structures. 2010, 47(2): 216−223.

[8] FRALDI M, GUARRACINO F. Evaluation of impending collapse in circular tunnels by analytical and numerical approaches [J]. Tunnelling and Underground Space Technology. 2011, 26(4): 507−516.

[9] FRALDI M, GUARRACINO F. Limit analysis of collapse mechanisms in cavities and tunnels according to the Hoek–Brown failure criterion [J]. International Journal of Rock Mechanics and Mining Sciences, 2009, 46(4): 665−673.

[10] QIN Chang-bin, SUN Zhi-bin, LIANG Qiao. Limit analysis of roof collapse in tunnels under seepage forces condition with three-dimensional failure mechanism [J]. Journal of Central South University, 2013, 20(8): 2314−2322.

[11] ZHANG Dao-bing, SUN Zhi-bin, ZHU Chuan-qu. Reliability analysis of retaining walls with multiple failure modes [J]. Journal of Central South University, 2013, 20(10): 2879−2886.

[12] HUANG Fu, ZHANG Dao-bing, SUN Zhi-bin. Influence of pore pressure effect on upper bound solution of collapse shape for square tunnel in Hoek-Brown media [J]. Journal of Central South University of Technology, 2011, 18(2): 530−535.

[13] LEE I M, NAM S W. Effect of tunnel advance rate on seepage forces acting on the underwater tunnel face [J]. Tunneling and Underground Space Technology, 2004, 19(3): 273−281.

[14] MOLLON G, DIAS D, SOUBRA A H. Rotational failure mechanisms for the face stability analysis of tunnels driven by a pressurized shield [J]. International Journal for Numerical and Analytical Methods in Geomechanics, 2011, 35(12): 1363−1388.

[15] MOLLON G, DIAS D, SOUBRA A H. Probabilistic analysis and design of circular tunnels against face stability [J]. International Journal of Geomechanics, 2009, 9(6): 237−249.

[16] WU Li-fen. Treatment for collapse of Dahuashan tunnel [J]. Technology of Highway and Transport, 2011, 15(1): 106−108. (in Chinese)

[17] WANG Lan, ZHANG Yong. Treatment for collapse of leigongshan tunnel [J]. Highways and Automotive Applications, 2004, 8(2): 98−100. (in Chinese)

[18] SUN Zhi-bin, ZHANG Dao-bing. Back analysis for soil slope based on measuring inclination data [J]. Journal of Central South University, 2012, 19(11): 3291−3297.

[19] HUANG Fu, ZHANG Dao-bing, SUN Zhi-bin, JIN Qi-yun. Upper bound solutions of stability factor of shallow tunnels in saturated soil based on strength reduction technique [J]. Journal of Central South University, 2012, 19(7): 2008−2115.

(Edited by HE Yun-bin)